

Investigating the RK Point of a Hamiltonian with Fractal Symmetries

Maxwell Siebersma

University of California Santa Barbara Department of Physics
Oregon State University Department of Physics

Faculty Advisor: Sagar Vijay

University of California Santa Barbara Department of Physics

(Dated: September 29, 2022)

In condensed matter systems, there exist certain Hamiltonians whose phase diagrams include a critical point known as the RK point. At this critical point, ground states of the system are given by equal amplitude superpositions of states connected by local flipping moves. The Hamiltonian explored in this paper, which describes the energetics on a triangular lattice with spin-1/2 degrees of freedom with a three-body interaction, is such a Hamiltonian with a phase transition at an RK point. This system in particular is known to possess an exotic Pascal's triangle symmetry with periodic boundary conditions. I explore the behavior of this system at the RK-point using exact diagonalization for small system sizes and using Markov-Chain Monte Carlo sampling to explore the behavior of larger systems. Monte Carlo sampling is used to generate a subset of states connected by local moves on these lattices and calculate correlation functions of interest for spins on varying sizes of lattice. I use the simulation to calculate three-point correlations on downward triangles on the lattice at various system sizes, as well as to calculate dimer-dimer correlations on the honeycomb lattice dual to the triangular lattice. Additionally, I include a proof of a symmetry possessed by lattices of side lengths divisible by 3, which leads to the vanishing of certain correlation functions on these lattices.

I. INTRODUCTION

A quintessential system of study in condensed matter theory is a set of spin-1/2 particles bound to the sites of a lattice. In addition to modelling a wide variety of physical materials, these systems are of interest due to the variety of emergent symmetries they may possess. Certain spin-1/2 systems contain exotic fractal symmetries, where conserved charges exist on fractal subsystems with non-integer dimension. Additionally, some systems exhibit critical points with changes in the overall symmetry by tuning parameters in the Hamiltonian of these systems. One notable type of critical point is the Rokhsar-Kivelson (RK) point, at which the ground states of a system are sets of equal amplitude superpositions of states connected by local moves. In this paper I investigate a Hamiltonian possessing both fractal symmetry and an RK point.

A. Pascal's Triangle Model

A system of recent interest is an array of spin-1/2 particles bound to the sites of a two-dimensional triangular lattice. A simple classical Hamiltonian (without quantum fluctuations) on this lattice is

$$H = -K \sum_{\nabla} \sigma_1 \sigma_2 \sigma_3 \quad (1)$$

with interactions of the Ising degrees of freedom on the lattice sites of downward triangles on the lattice, as illustrated in figure 1. This type of model was originally conceived as a means of investigating spin glasses [1], and contains three-spin interactions over the lattice. Importantly, this model contains a fractal symmetry. This is a consequence of the three-spin interaction in the Hamiltonian; by flipping spins in a Sierpinski fractal, either two or zero spins are flipped on every

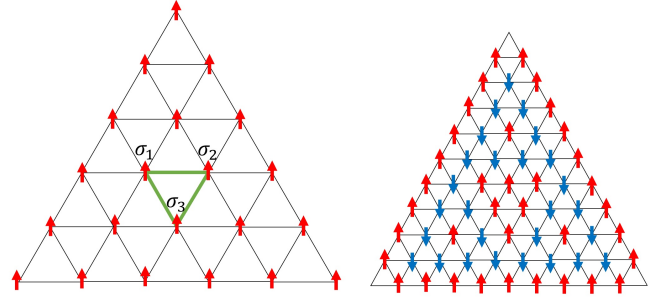


FIG. 1. A representation of the triangular lattice with Pascal's triangle symmetries. Spins interact on the sites of a downward triangle on the lattice. This system contains a fractal symmetry, where spin 1/2 lattice sites can be flipped in the pattern of a Sierpinski fractal.

downward triangle, as illustrated in figure 1 [2]. As recently discovered, this lattice in fact contains a more general $U(1)$ symmetry, with different symmetries for lattices with spin degrees of freedom of prime order [3]. These symmetries follow the symmetries of Pascal's triangle, modulo the spin degrees of freedom. This underlying Pascal's triangle symmetry reappears on such triangular lattices with three-spin interactions as appear in this paper.

B. Rokhsar-Kivelson Points

The Rokhsar-Kivelson (RK) critical point was first explored by Rokhsar and Kivelson in the context of the quantum dimer model [4]. This system consists of dimers which cover the sites of a two dimensional square lattice. The Hamiltonian of this system is

$$H = \sum -t(|\uparrow\uparrow\rangle\langle\downarrow\downarrow| + h.c.) + v(|\uparrow\uparrow\rangle\langle\uparrow\uparrow| + |\downarrow\downarrow\rangle\langle\downarrow\downarrow|). \quad (2)$$

where the kets symbolize states with dimers on opposing sides of squares on the lattice [5]. While the ground states cannot be found exactly in general, they can be found when $v = t$, where the Hamiltonian can be reexpressed as

$$H = \sum -t(|\uparrow\downarrow\rangle - |\downarrow\uparrow\rangle)(\langle\uparrow\downarrow| - \langle\downarrow\uparrow|) \quad (3)$$

The ground states at this critical point are given by the equal amplitude superposition of sets of states which can be reached by local "flip moves" on the lattice. In the case of the dimer model, these moves are flipping the dimers on square plaquettes with opposing dimers [5]. These ground states are similar in form to partition function in classical statistical mechanics because of the equal amplitude sum. However, generating the component of states connected by local spin flips is a nontrivial task.

C. Hamiltonian with an RK Point on the Triangular Lattice

To bring together the notions of the Pascal's triangle model with RK points, consider again the spin-1/2 degrees of freedom on the triangular lattice. This paper is built around the Hamiltonian

$$H = t \sum_{\nabla} [|\phi_{\nabla}^{\uparrow}\rangle - |\phi_{\nabla}^{\downarrow}\rangle] [\langle\phi_{\nabla}^{\uparrow}| - \langle\phi_{\nabla}^{\downarrow}|] + h \sum_{\nabla} [|\phi_{\nabla}^{\uparrow}\rangle \langle\phi_{\nabla}^{\uparrow}| + |\phi_{\nabla}^{\downarrow}\rangle \langle\phi_{\nabla}^{\downarrow}|] \quad (4)$$

where $|\phi_{\nabla}^{\uparrow}\rangle = |\uparrow_1, \uparrow_2, \uparrow_3\rangle$ and $|\phi_{\nabla}^{\downarrow}\rangle = |\downarrow_1, \downarrow_2, \downarrow_3\rangle$ for the three lattice sites on a plaquette, and the sum runs over every downward triangle on the lattice. We will fix t to be a positive constant, while h is a tunable parameter. This Hamiltonian is built of projection operators on plaquettes with spins all aligned, which will be referred to as "flippable." If a plaquette is not flippable, the projector corresponding to it for that configuration will equal zero. As such, if h is positive, the ground states of the Hamiltonian will be those where every plaquette is not flippable. However, when h goes to zero, the Hamiltonian becomes

$$H = t \sum_{\nabla} [|\phi_{\nabla}^{\uparrow}\rangle - |\phi_{\nabla}^{\downarrow}\rangle] [\langle\phi_{\nabla}^{\uparrow}| - \langle\phi_{\nabla}^{\downarrow}|] \quad (5)$$

which is the form of the Hamiltonian for an RK point. While the ground states in the frozen configuration persist, a much larger landscape of groundstates appears, corresponding the superposition of sets of states connected by local flip moves. For this system, the local flip move at the RK point is flipping the spins on a downward triangle plaquette. It is the goal of this paper to explore the nature of the RK point, understood using these local flips. Assuming periodic boundary conditions on the triangular lattice, the Hamiltonians for small system sizes, such as the 3×3 and 4×4 lattices can be solved exactly using exact diagonalization. However, larger lattices have too large a Hilbert space of states to be solved exactly; instead classical Monte Carlo methods can be used to characterize these systems.

II. EXACT DIAGONALIZATION

A. Representing Lattice Configurations

In order to diagonalize this Hamiltonian, it is first necessary to develop a consistent scheme for organizing the spin states on the lattice. For a square lattice with periodic boundary conditions of side length of n , there will be a total of n^2 downward triangles on the lattice. Each plaquette corresponds to a unique lattice site; we will use the lattice site at the top left corner. The lattice sites can be enumerated as shown in figure 2. Using this convention, the lattice sites on a given downward plaquette i are given by

$$a = i \quad (6)$$

$$b = (i \bmod (n) + 1) \bmod (n) + (i - i \bmod (n)) \quad (7)$$

$$c = (b - n) \bmod (n^2). \quad (8)$$

These nearest neighbor relations can then be stored in an array to be accessed at a later point. For n^2 spin-1/2 particles on the lattice, there are a total of 2^{n^2} possible configurations of spins on the lattice in the S_z basis. For convenience, these states can be enumerated by taking the numbering scheme shown in figure 2 and assigning each lattice position a value of 1 if it is spin-up and 0 if it is spin down. The S_z basis states may be enumerated by interpreting these values as binary numbers and converting them to base 10 integers. For example, on the 2×2 lattice, the all-down state 0000 is assigned the number 0, and the all-up state 1111 is assigned the number 15.

B. Sparse Structure and Diagonalization Procedure

The size of the Hilbert space of spin states increases exponentially with the number of lattice sites; as such, calculating the full Hamiltonian is a cumbersome task even for small system sizes. Fortunately, this particular Hamiltonian has a very sparse structure, making it so that only nonzero values need to be stored. I computed this Hamiltonian in Python using the package *scipy.sparse*, storing the Hamiltonian as a CSR matrix. Additionally, since the Hamiltonian is necessarily Her-

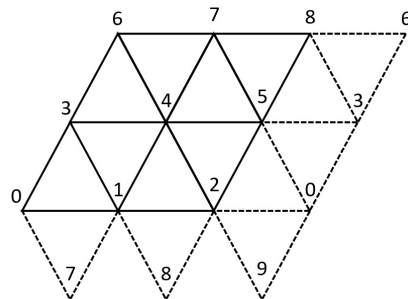


FIG. 2. 3×3 triangular lattice with periodic boundary conditions. This figure shows the numbering scheme used to represent positions on a given lattice. The lattice sites on any given plaquette i are given by equations 6-8.

mitian, only the upper triangular portion of the matrix must be calculated directly. In the S_z basis, each row and column of the Hamiltonian corresponds to a spin state on the lattice; these are enumerated according to the previous section. We can interpret the projection operators constituting the Hamiltonian in equation 5 as follows: If the states of the row and column are the same, the value of the matrix entry is the number of plaquettes on the lattice. If the states of the row and column differ by a single plaquette flip, the matrix entry is assigned the value -1 . Using this general scheme, the Hamiltonian can be built as a sparse matrix. The *scipy.sparse* package can then be used to compute the eigenvalues and eigenvectors of the matrix.

C. Ground States

By using this process, we are interested in computing the groundstates at the RK point. Each ground state has an energy eigenvalue of 0 and is given by a vector where each non-zero entry corresponds to the set of states connected by local flip moves. However, this basis of ground states will not be given by the computational output due to the large ground state degeneracy at the RK point combined the numerical processes used to calculate eigenvectors. Nevertheless, the vectors as interpreted using the RK point and the vectors calculated numerically will both be valid spanning sets for the space of ground states. Accordingly, all of the computed vectors can be composed into a basis of RK states. Since every RK basis vector is an equal amplitude sum of spin states, we may simply iterate through the given ground state vectors and pick out entries with equal values; once normalized these will form the RK basis. We can check to see that the resultant set of vectors from this process gives the correct number of ground states. Every configuration of spins on the lattice will belong to one and only RK component.

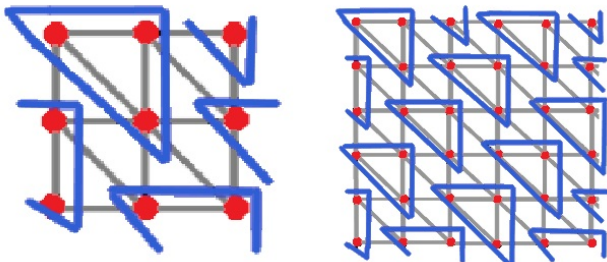


FIG. 3. Downward triangle tiling on $3k \times 3k$ lattices. On the 3×3 lattice, the shown tiling scheme can tile the lattice with downward triangles, meaning that every spin on the lattice can be flipped from up to down. Due to the periodic boundary conditions, this tiling scheme exists on all $3k \times 3k$ lattices. For example, the 6×6 tiled lattice is shown to the right.

III. THE ALL-UP COMPONENT ON $3k \times 3k$ LATTICES

Interestingly, the triangular lattices with sidelengths of multiple three have a particular symmetry which elucidates some of their unique properties. Denote the configuration on a lattice with all spins oriented up as $|C_\uparrow\rangle$. Recall that the ground states at the RK point are given by the equal amplitude superposition of configuration states connected by local flip moves, i.e.

$$|\Omega\rangle = \frac{1}{\sqrt{N_s}} \sum_{i|\Omega} |C_i\rangle \quad (9)$$

Therefore, any state $|C_i\rangle$ within the same component as $|C_\uparrow\rangle$ can be reached by some sequence of plaquette flip operations $\prod f_z$ such that $|C_i\rangle = \prod f_z |C_\uparrow\rangle$. However, on the 3×3 lattice, there is an exact tiling of downward triangles, such that every spin in the all-up component can be flipped exactly once. This tiling of triangles is shown in figure 3. Moreover, because of the periodic boundary conditions on the lattice, this tiling scheme can be extended to any $3k \times 3k$ lattice for $k \in \mathbb{N}$. This tiling demonstrates that for any such $3k \times 3k$ lattice, there exists a sequence of downward plaquette flips $\prod f_T$ on the tiled downward triangles such that

$$|C_\downarrow\rangle = \prod f_T |\uparrow\rangle \quad (10)$$

where $|C_\downarrow\rangle$ is the lattice configuration with all spins oriented down. This fact implies that for any configuration $|C_i\rangle$ in the all-up component, the "anti-configuration" $|C'_i\rangle$ with every spin reversed is also in the all-up component. To prove this, the sequence of flip operations $\prod f_z$ to reach $|C_i\rangle$ reduces to some product of spin flips on the all up lattice, which can be expressed as

$$\mathcal{U} = \prod f_z = \prod_k \sigma_k^x \quad (11)$$

\mathcal{U} corresponds to a valid sequence of plaquette flips on the all-up configuration, so the same set of flips can be applied to the all-down configuration. This operation will yield the exact opposite spin configuration as $|C_i\rangle$. Thus, every configuration of spins $|C_i\rangle$ in the all-up component of a $3k \times 3k$ lattice will be connected by spin flips to its spin reversal $|C'_i\rangle$, where $\sigma_n^i = \sigma_n^{-i}$ for all spins n on the lattice.

As a corollary, any correlation function consisting of the product of an odd number of distinct Ising spins will go to zero for the all-up component on a $3k \times 3k$ lattice. This correlation function can be expressed as

$$\langle \prod_j^{2n+1} \sigma_j \rangle = \langle \Omega | \sigma_1 \sigma_2 \dots \sigma_{2n+1} | \Omega \rangle, \quad (12)$$

where $|\Omega\rangle$ is the ground state associated with the all-up component and all spins σ_j are distinct. This can be expanded with the knowledge that every state in the component also has its spin reversal also in the component.

$$\langle \prod_j^{2n+1} \sigma_j \rangle = \langle \Omega | \sigma_1 \sigma_2 \dots \sigma_{2n+1} \left(\frac{1}{2\sqrt{N_s}} \sum_{i|\Omega} |C_i\rangle + |C'_i\rangle \right) \quad (13)$$

$|C'_i\rangle$ has the opposite spin configuration as $|C_i\rangle$, which implies that

$$\left(\prod_j^{2n+1} \sigma_j\right)(|C_i\rangle + |C'_i\rangle) = \sigma_1^i \sigma_2^i \dots \sigma_{2n+1}^i |C_i\rangle + (-1)^{2n+1} \sigma_1^i \sigma_2^i \dots \sigma_{2n+1}^i |C_i\rangle. \quad (14)$$

From here, the inner product will evaluate to zero, since $\langle \Omega | C_i \rangle = \langle \Omega | C'_i \rangle = 1/\sqrt{N_s}$. It is important to note that this result only holds true for correlations on the all-up component, only on $3k \times 3k$ lattices, and only for a product of an odd number of spins. However, these correlation functions will evaluate to zero regardless of where on the lattice the spins are chosen from.

IV. MONTE CARLO SIMULATIONS

In order to gain information on larger lattices, it is impractical to attempt to deal with the Hamiltonian as a whole. However, a Markov chain Monte Carlo simulation can be used to sample states connected by local flips on the lattice. The ground states at the RK point lend themselves to simple investigation through Monte Carlo techniques. Since the ground states in question are an equal amplitude superposition of states, they are characteristically similar to the partition function in classical statistical mechanics. As such, classical Monte Carlo methods can be used to sample through these connected states [6]. Using these simulations, we can measure correlation functions of interest in order to obtain information about the system.

A. Structure of the Monte Carlo Simulation

To begin, it is useful to analyze the component of states beginning with the all-up lattice. This state is simplest to analyze and most general because it is isotropic; there are no "preferred directions" on states connected to the all-up state. In turn, for any correlation function we wish to measure on the lattice, we may average this over measurements on all downward triangles without loss of generality. The initial state can be stored as a vector where each element in the vector corresponds to a spin on the lattice. As we run through the simulation, at each time step we randomly choose a single plaquette. If the three spins on this triangle corresponding to this plaquette are the same, we flip them, which is accomplished by multiplying all three by -1 . If the spins are not all in the same orientation, we simply continue on to the next time step. It is important that the simulation continues in the case of unsuccessful flips in order to maintain detailed balance. Otherwise, there would be biases towards certain states based on the number of flippable plaquettes; this would not sample correctly in order to build an equal amplitude superposition.

Additionally, using the property proved in Section III, it is possible to implement a global update for $3k \times 3k$ lattices. We can assign a separate random variable which, at any given step, has some probability of choosing to perform a global

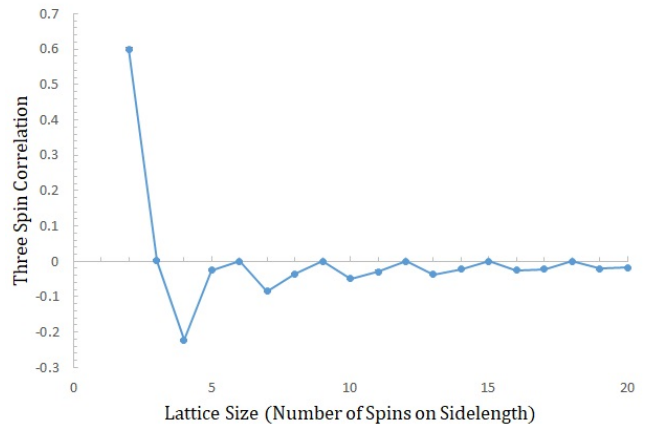


FIG. 4. Three-spin correlation with increasing lattice size. In the thermodynamic limit, this correlation function tends towards zero. For lattices of size $3k \times 3k$, the correlation is exactly zero.

update instead of a local update. When this occurs, the every spin on the lattice is reversed, as is allowed on this specific size of system. This is ideal because it allows us to move to a disparate part of the network of states connected by local moves, as opposed to plaquette flips, which move around this network locally. This process allows for more ergodic sampling of the network.

At given points in time, we can sample correlation functions given by some set of spin orientations. In order to maintain ergodic sampling, one should not sample at every time step in the simulation, but rather after some designated interval of time τ . There will be less correlation between two given states the longer the amount of time allotted between correlation measurements.

B. Three-Spin Correlation Function

One of the simplest correlation functions to find on the lattice is the correlation function of three spins on the site of a downward triangle, written as

$$C_{3s} = \langle \sigma_1 \sigma_2 \sigma_3 \rangle. \quad (15)$$

While this refers to the three-spin correlation of a single plaquette, the isotropy of the all-up state means that this correlation will be the same on all plaquettes in this RK ground state. Accordingly, we can obtain more accurate results from the Monte Carlo sampling by measuring this correlation over all plaquettes and taking the average:

$$C_{3s} = \frac{1}{N_{\nabla}} \sum_{\nabla} \langle \sigma_1 \sigma_2 \sigma_3 \rangle. \quad (16)$$

We may compute this correlation function on various sizes of lattice, as shown in figure 4.

The three-spin correlation function goes to zero at lattice with side length $3k$ spins, as expected from the analytic results

in Section III. Additionally, the results for small system sizes match with those computable from exact diagonalization. In general, as system size increases towards the thermodynamic limit, the three-spin correlation tends towards zero.

C. Dimer-Dimer Correlations

On the triangular lattice, there exists a dual honeycomb lattice, where the sides of each hexagonal element pass through the bond between two spins on the triangular lattice (Myerson-Jain et al 2022). We may assign dimers to links on the honeycomb lattice corresponding to whether or not the two spins they pass through are in the same orientation, as illustrated in figure 5. For any dimer, we can assign the projection operator

$$P_D = \frac{1 + \sigma_1 \sigma_2}{2} \quad (17)$$

which takes a value of 1 if the two spins are aligned and 0 if not. It is of interest to measure the correlation function between two such dimer projections, as expressed by

$$\langle P_i P_j \rangle = \left(\frac{1 + \sigma_{i1} \sigma_{i2}}{2} \right) \left(\frac{1 + \sigma_{j1} \sigma_{j2}}{2} \right) \quad (18)$$

and varying the relative positions of the two dimers across the lattice. It is known that above the RK point, dimer-dimer correlations decrease as a power law as dimers increase in distance across the lattice. Additionally, dimer-dimer correlations may vary depending on whether the dimers in question are of aligned or unaligned orientation.. To investigate this correlation function, I ran the Monte Carlo simulation on a 60×60 lattice and once again measured and averaged over all sites on the lattice. Due to periodic conditions, the maximum measurable distance in a given direction is 30 lattice sites. The results for same and mixed orientation dimer-dimer correlations are shown in 6. As can be seen, although there is a low correlation between any two dimers at any distance, there is a persistent long range correlation between dimers that does not diminish at increasing distances on the lattice. The difference in behavior of the correlation function between the RK point and frozen phase suggests that the RK point of this Hamiltonian corresponds to a phase transition. This phase allows for long range correlations, as demonstrated with dimer-dimer correlations. Intriguingly, this cor-

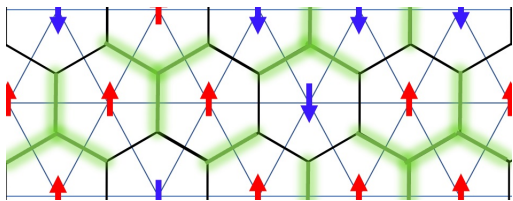


FIG. 5. Dimers on the dual honeycomb lattice. Under the most basic interpretation, there exists a dimer on every segment of the dual lattice which passes through a segment connecting two aligned spins on the triangular lattice.

Average Dimer-Dimer Correlation on 60×60 Lattice by Distance (Connection Subtracted)

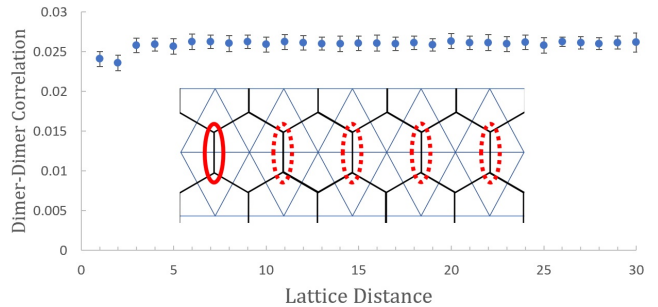


FIG. 6. Dimer-Dimer Correlation on 60×60 lattice with same orientation dimers. For this plot, the connection term between the two projection operators of 0.25 is subtracted. The inset image shows how the dimers measured vary in space across the lattice. Error bars are generated from standard deviation across trials.

relation seems to break down at shorter distances on the lattice. For same orientation dimers, the correlation is actually less for dimers within one or two lattice sites than for further separations. While it appears that on a large scale correlations become uniform, local effects possess more non-trivial behavior.

D. Trimers as Monomers

To further explore the nature of long and short range behavior of correlation functions on the lattice, we consider now a different set of correlations corresponding to the dual honeycomb lattice. For any given lattice site on the dual lattice, there are two possibilities: either there is a single dimer at the site or there are three dimers connected together, the latter we can refer to as a 'trimer.' When a trimer takes the shape ' λ ', this corresponds to a flippable downward triangle. For a given trimer, we can define the projection operator

$$P_\lambda = \left(\frac{1 + \sigma_a \sigma_b}{2} \right) \left(\frac{1 + \sigma_a \sigma_c}{2} \right) \left(\frac{1 + \sigma_b \sigma_c}{2} \right) \quad (19)$$

using the three projection operators corresponding to the constituent dimers. While the trimer/dimer representation is worth consideration, it can be altered in order to gain more insight into dimer-dimer correlations. For every lattice site on the dual lattice that corresponds to a trimer, we may instead represent it as a monomer on that lattice site, as illustrated in figure 7. This alternate picture of the dual lattice gives us a monomer-dimer covering corresponding to a spin configuration on the lattice. We may thus alter our dimer-dimer correlation function to exclude any dimers which form part of a trimer, since in the new representation, these correspond to monomers and thus would not have an associated trimer. This is most easily implemented into the Monte Carlo simulation by adding an additional condition which checks if neighboring spins are also aligned to the dimer. This added degree of stringency can lead to greater insights into how dimer-dimer

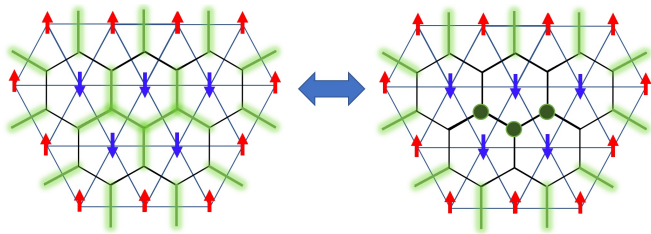


FIG. 7. Transitioning from trimers to monomers on the honeycomb lattice. We replace each trimer on the lattice with a monomer, indicated by a dot on the given lattice site. With this, we have a new picture of the dual lattice with dimers and monomers corresponding to each lattice pair of spins.

correlations vary with distance. It is worth noting that this new correlation function reduces to equation 18 in the frozen phase, since there are no aligned triangles in this phase.

Figure 8 gives the results of the Monte Carlo simulation measuring this new dimer-dimer correlation with dimers varying in distance, for both aligned and unaligned dimers. These are enlightening in showing a greater degree of spatial dependence than was obvious from the earlier correlaiton. At long distances, both aligned and unaligned dimer correlations converge towards a constant value. However, at shorter distances, the correlations diverge, becoming larger for unaligned dimers and smaller for aligned dimers. While this is not necessarily the same $|\mathbf{r}|^{-1}$ dependence expected in the frozen phase, this observed spatial dependence may offer more insight into the order of the RK point.

V. CONCLUSIONS

In this paper I have investigated the RK Point of a Hamiltonian on a triangular lattice with a fractal symmetry. This Hamiltonian has a large ground state degeneracy, with each ground state corresponding to a set of spins state on the lattice connected by local plaquette flips. For small lattice sizes, I have briefly laid out my process for constructing the Hamiltonian computationally and using exact diagonalization to solve numerically for the set of ground states. Following this, I proved the existence of a \mathbb{Z}^2 symmetry on the set of $3k \times 3k$ lattices, leading to the vanishing of certain correlation functions on these lattices. I used Monte Carlo methods in order to explore the RK point on larger lattices and obtain numerical results of correlation functions. Among these, I found that dimer-dimer projections possess long range correlations at the RK point, implying a the possibility of a phase transition at the RK point.

Different types of correlation functions may be useful to truly understand the order of this Hamiltonian's RK point. In particular, off-diagonal operators on regions of equilateral triangles were explored as a possible route of inquiry. However, the challenges posed by off diagonal operators were difficult to rectify using Monte-Carlo methods, since these correlations require analyzing and comparing many different states in the ground state manifold. However, this path may prove to be

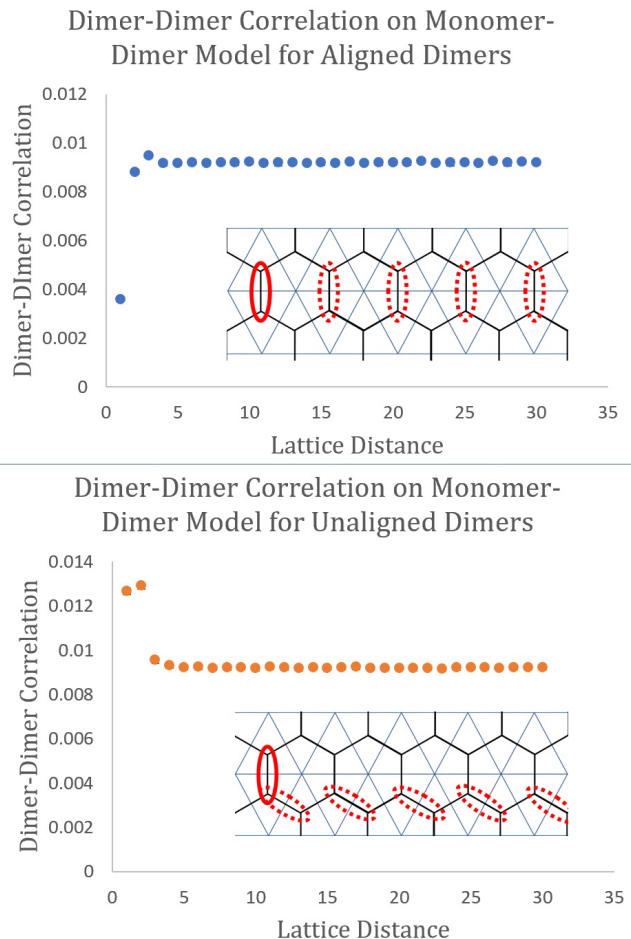


FIG. 8. Graphs showing the dimer-dimer correlation over distance factoring in to disclude monomers from the correlation. The top plot shows the correlation on aligned dimers, while the bottom plot shows this for unaligned dimers. Error bars are generated from standard deviation across trials.

fruitful in further exploration of this RK point if computational issues can be rectified.

We wish to eventually better understand the dynamics of flippable triangles under this Hamiltonian. The manner in which these flippable triangles are able to move about the lattice is not completely understood, and more work is needed to better describe this. Further, the ground states of this Hamiltonian beyond the RK point, where h and t have opposite sign in equation 4, are still not well understood. While this investigation into the RK point may hint at a different phase beyond this point, more concrete results are needed. In total, fractal symmetries in condensed matter systems are a new frontier of exploration and could exhibit many yet unknown exotic properties. This work lays the groundwork for the exploration of a Hamiltonian which could lead to novel insights into the behavior of these systems.

ACKNOWLEDGMENTS

I would like to thank my advisor, Dr. Sagar Vijay and my graduate mentor, Zhehao Zhang for their mentorship throughout this project. Their help and guidance was indispensable, allowing me to directly contribute to research in condensed matter theory. I would also like to thank the REU site direc-

tor, Dr. Sathya Guruswamy, for coordinating this program and giving structure to this summer experience. I also cannot neglect to acknowledge all of my fellow REU participants for their support throughout and making this such a memorable experience. In addition, I would like to thank the National Science Foundation for sponsoring and facilitating this REU program. This work was supported by NSF REU grant PHY-1852574.

-
- [1] M. E. J. Newman and C. Moore, *Phys. Rev. E* 60, 5068 (1999), URL <https://link.aps.org/doi/10.1103/PhysRevE.60.5068>.
- [2] Zhou, Zheng, Zhang, Xue-Feng, Pollmann, Frank, You, Yizhi. (2021). Fractal Quantum Phase Transitions: Critical Phenomena Beyond Renormalization, arXiv:2105.05851
- [3] Nayan E. Myerson-Jain, Shang Liu, Wenjie Ji, Cenke Xu, and Sagar Vijay *Phys. Rev. Lett.* 128, 115301 – Published 14 March 2022
- [4] D. S. Rokhsar and S. A. Kivelson, *Phys. Rev. Lett.* 61, 2376 (1988).
- [5] Moessner, Roderich, and Kumar S. Raman. "Quantum dimer models." *Introduction to Frustrated Magnetism*. Springer, Berlin, Heidelberg, 2011. 437-479.
- [6] Syljuåsen, Olav F. "Random walks near Rokhsar-Kivelson points." *International Journal of Modern Physics B* 19.12 (2005): 1973-1993.